

## High T<sub>g</sub> Polyimides

Kathy Chuang NASA Glenn Research Center, Cleveland, OH 44135

### Table of Contents

- I. Introduction
- II. PMR-Type Polyimides
- III. Polyimides Based on Substituted Benzidines
  - A. High T<sub>g</sub> Thermosetting Polyimides Based on Substituted Benzidines
    - 1) Resin properties
    - 2) Composite fabrication and properties
  - B. Thermoplastic Polyimides Based on Substituted Benzidines
    - 1) Polyimide Fibers
    - 2) Stereochemistry of substituted benzidines
    - 3) Polyimide Films
- IV. Endcap Chemistry in Imide Oligomers
- VI. Conclusion

This report is a preprint of an article submitted to a journal for publication. Because of changes that may be made before formal publication, this preprint is made available with the understanding that it will not be cited or reproduced without the permission of the author.

## I. INTRODUCTION

The use of high temperature polymer matrix composites in aerospace applications has expanded steadily over the past 30 years, due to the increasing demand of replacing metal parts with light weight composite materials for fuel efficiency and bigger payloads in the aircraft and the space transportation vehicles. Polyimide/carbon fiber composites, especially, have been regarded as major high temperature matrix materials, based on their outstanding performance in terms of heat resistance, high strength-to-weight ratio and property retention compared with epoxies (177 °C/350 °F) and bismaleimides (232 °C/450 °F) [1]. Traditional, thermoplastic polyimides were prepared from dianhydrides and diamines in N-methyl-2-pyrrolidinone (NMP) at room temperature to form the polyamic acids, which were then imidized at 150 °C to yield polyimides. However, the high-boiling solvent (NMP, BP= 202 °C) is very difficult to remove, leading to the formation of voids during composite fabrication. In the early 1970's, PMR addition curing polyimides with reactive endcaps were developed at the Lewis Research Center (renamed NASA Glenn) to ensure the easy processing of imide oligomers in methanol during composite fabrication.

## II. PMR-Type Polyimides

Using the **PMR** approach (*in-situ* polymerization of monomer reactants), PMR-15 [2] was formulated from 3,3',4,4'-benzophenonetetracarboxylic dimethyl ester (BTDE), methylene dianiline (MDA) with *endo-cis*-bicyclo[2.2.1]-5-heptene-2,3-dicarboxylic acid, methyl ester (nadic ester, NE) as the reactive endcap (Fig. 1). The ratio of BTDE: MDA: NE corresponded to  $n : n + 1 : 2$ , where  $n$  is the repeat unit of the oligomer. For PMR-15,  $n$  equals 2.087, which essentially yields a formulated molecular weight of 1500 g/mole. The formulated molecular weight (FMW) of a PMR polyimide can be calculated as follows:

$$\text{FMW} = 2 (\text{MW of endcap}) + n (\text{MW of dianhydride derivative}) \\ + (n + 1) (\text{MW of diamine}) - 2 (n + 1) (\text{MW of water} + \text{MW of alcohol})$$

The imidized oligomers with the nadic endcap are usually only partially soluble in most solvents, including NMP; therefore, it is often difficult to assess the number average ( $M_n$ ) molecular weight of the PMR oligomers by gel permeation chromatography (GPC). As shown in Figure 1, the monomers were first dissolved in low-boiling methanol to form a solution, which was then painted on the surface of various carbon fiber or fabric reinforcement to form prepreg. The monomers were polymerized *in-situ* within the stacks of prepreps upon heating to form low molecular weight oligomers [3], which facilitate easier processing of laminates. At the final stage of curing, the reactive nadic endcaps of the imide oligomers were crosslinked under pressure (200 psi) and heat (316 °C/600 °F) to form polyimide composites. The ease of alcohol removal during processing is in the order of methanol > ethanol > isopropanol, following the vapor pressure of these alcohols. Also the reaction mechanism indicated that the corresponding acid ester first reverted to the dianhydride in the same order before reacting with the diamine [4]. Solution stability of the monomer solutions and the shelf life of prepreps follow in the

order of isopropyl ester > ethyl ester > methyl ester, because of the slower reaction between isopropyl esters of dianhydrides and the nadic endcap with diamines that prevents the aging and precipitation of the resin solution [5]. The curing of nadic endcaps is very complicated and is believed to involve several possible pathways including the retro-Diels-Alders reaction, the addition of cyclopentadiene to either bismaleimides or the unreacted nadic unit [6-10], and a simple curing of double bonds of the nadic endcap [11].

PMR-15 offers easy processing and good property retention at a reasonable cost; thus, it is widely used in aircraft engine components and has been recognized as the state-of-the-art composite material for long-term use (thousands of hours) at 288 °C (550 °F). However, methylene dianiline (MDA) in PMR-15 is a known toxin to the liver; therefore, it requires stringent safety regulation. Over the years, analogs of PMR-15 involving replacement of MDA with various diamines have been investigated:

A) Evaluation of PMR polyimides based on nadic ester, dimethyl esters of pyromellitic dianhydride (PMDA), 3,3',4,4'-benzophenonetetracarboxylic dianhydride (BTDA) and 4,4'-(hexafluoroisopropylidene)diphthalic anhydride (HFDA) [12,13] are summarized in Table 1. These resin and composite screening studies have revealed the following:

- 1) The thermo-oxidative stability of PMR polyimides increased with decreasing aliphatic content obtained by increasing the formulated molecular weight as a result of a lower percentage of the aliphatic nadic endcap.
- 2) PMR polyimides containing diamines with benzylic linkages (-CH<sub>2</sub>-, -CHPh) between two phenyl rings, such as methylenedianiline (MDA) and diaminotriphenylmethane (DAPTM), displayed better thermo-oxidative stability than that of the non-benzylic diamines. In addition, polyimides based on HFDE and *p*-phenylenediamine (no linkage to degrade) exhibited excellent thermo-oxidative stability comparable to that of PMR resins with benzylic linkages.
- 3) Dianhydrides played a secondary role in the thermo-oxidative stability of PMR polyimides after the benzylic effect in the diamines. The stability of PMR polyimides derived from dianhydrides were in the order of HFDA > PMDA > BTDA. However, PMDA-containing PMR polyimides were usually difficult to process.
- 4) Postcure in air increased the T<sub>g</sub>'s of thermosetting polyimides.

B) Use of diamines with ether, isopropylidene [-(CH<sub>3</sub>)<sub>2</sub>C-], hexafluoroisopropylidene [-(CF<sub>3</sub>)<sub>2</sub>C-] and 2,2' - bis([4-(4-aminophenoxy)phenyl]hexafluoropropane (4-BDAF) linkages [14,15]:

Several of these diamine modifications have been fabricated into composites successfully, such as 3,4'-oxydianiline in LARC-RP-46 [16,17], 2,2-bis[4-(4-aminophenoxy)phenyl]propane in AMB-21 [18,19], bisaniline P and Bisaniline M [20, 21] (Table 2). Although the ether and isopropylidene linkages tend to enhance the processability, these flexible linkages often lower the glass transition temperature (T<sub>g</sub>) and reduce thermo-oxidative stability [22] of the resulting polyimides, relative to that of PMR-15. The *m*-linkage in the Bisaniline M contributes to the enhanced solubility of the diamine in alcohol and improves the processability of the resin.

However, the *m*- linkage in bisaniline M lowers the  $T_g$  of the resulting polyimide as compared to the *para*-linkage in bisaniline P.

C) Use of 3-ring aromatic diamines with either methylene ( $-\text{CH}_2-$ ) or carbonyl ( $\text{C}=\text{O}$ ) linkages [23]:

As shown in Table 3, the methylene linkage is more thermally stable than the carbonyl as evidenced by the lower weight loss during isothermal aging at 288 °C. However, the carbonyl linkage usually yields higher  $T_g$  in the cured polyimides. *Meta* linkages generally contributed to better resin melt-flow, but lower  $T_g$ 's and poorer thermo-oxidative stability in polyimides than the corresponding *para* catination.

D) Use of 4-ring aromatic diamines containing methylene ( $-\text{CH}_2-$ ), carbonyl ( $\text{C}=\text{O}$ ), ether and sulfur linkages [24]:

The methylene and carbonyl linkages exhibited lower weight loss than the ether or sulfur linkages. However, 4-ring aromatic diamines were not very soluble in alcohol solvents, harder to process and afforded polyimides with lower  $T_g$ 's than 3-ring diamines (Table 4).

E) Second Generation of PMR-Polyimides based on HFDA:

To increase the high temperature stability of PMR-15 beyond 288 °C (550 °F), a second generation of PMR polyimide, PMR-II-50 [25], was developed for 315 °C (600 °F) applications. PMR-II-50 was formulated with 4,4'-(hexafluoroisopropylidene)diphthalic acid, dimethyl ester (HFDE), *p*-phenylenediamine (*p*-PDA) with  $n = 9$ , and the nadic ester (NE) as the endcap. Upon curing, PMR-II-50 yielded a backbone similar to DuPont's thermoplastic polyimide Avimid N<sup>®</sup> (i.e. NR-150B2) that was based on HFDA and a 95/5 mixture of *p*-PDA and *m*-PDA [26]. However, the approach of using the oligomers produced with endcap in methanol offered improved processability over the thermoplastic polyimide in NMP. Since it is known that the aliphatic components of the nadic endcap contributed to the thermo-oxidative degradation of the PMR polyimides [27], other efforts to modify PMR-II-50 were concentrated on changing the endcap (Table 5) from the nadic ester to other endcaps containing aromatic moieties; such as 4-amino-[2.2]-*p*-cyclophane (CYCAP) [28], *p*-aminostyrene (V-CAP) and 4-phenylethynylphthalic acid, methyl ester (PEPE) [29] and 3-phenylethynylaniline (PEA) [30]. Another approach was to reduce the amount of nadic endcaps used to half of that in PMR-II-50 as demonstrated in AFR700-B polyimide [31]. The  $T_g$ 's of these polyimides ranged from 330-380 °C after postcure at 371 °C in air (Table 6). Since these polyimides were all composed of 6F-dianhydride and *p*-PDA as the backbone except variations with ~10 % of different endcaps, they all exhibited comparable weight loss [32] and similar mechanical properties (Table 6). However, the ease of processing for the polyimide composites with various endcaps followed the order of phenylethynyl > *p*-aminostyrene > nadic ester. The curing of phenylethynyl group is slower than the nadic endcap, and the oligomers terminated with either phenylethynyl or vinyl groups exhibited more plasticity than the nadic endcap during processing. However, the curing of *p*-aminostyrene endcap usually produced polyimides with lower  $T_g$ 's than the corresponding nadic endcap. As shown in Table 6 and 7, higher  $T_g$  and optimal mechanical strength could be achieved in polyimide composites by air postcure at 371 °C

for 20 hours followed by nitrogen postcure at 399 °C (750 °F) for an additional 20 hours [29, 33]. Nitrogen postcure was believed to involve reactions of free radicals trapped within the polyimide composites [34]. However, prolonged nitrogen postcure at 399 °C for 40 hours eventually resulted in lower mechanical strength, due to the degradation of polyimides at elevated temperature as shown in Table 7.

#### F. Other modified PMR polyimides [35,36]

To improve the processability, a solventless PMR nadimide resin (LARC-160) was formulated by replacing the 4,4'-methylenedianiline in PMR-15 with a liquid mixture of isomeric polyamines (Jeffamine 22) [37] for hot-melt processing, but its thermo-oxidative stability was not as good as PMR-15. In addition, N-phenylnadimide was used as an additive (4-20 molar %) to improve the flow of PMR-15 for easier processing without sacrificing its high temperature capability [38]. Interpenetrating networks of the thermosetting PMR-15 resin mixed with other thermoplastic polyimides; such as NR-150B2 (6F dianhydride with 5/95 ratio of *m*-phenylenediamine and *p*-phenylenediamine), were also investigated in order to increase the toughness of PMR-15 [39]. A variation of PMR-15 using 4,4'-oxydianiline and the biphenylene endcap along with the diester of 3,3',4,4'-benzophenone dianhydride (BTDE) yielded lower  $T_g$ 's and poorer thermal stability than PMR-15 [40].

### III. Polyimides Based on Substituted Benzidines

During the 1980's, non-coplanar 4,4'-biphenyldiamines (i.e. 2,2'-substituted benzidines) received lots of attention in the field of polyamides and polyimides. Polyamides based on 2,2'-bis(trifluoromethyl)benzidine were shown to display optical transparency and high birefringence [41]. Furthermore, polyimides based on non-coplanar benzidines were shown to exhibit high thermo-oxidative stability [42] and optically clear films with low coefficients of thermal expansion (CTE) suitable for electronic applications [43].

#### A. High $T_g$ Thermosetting Polyimides Based on Substituted Benzidines

##### 1) Resin Properties

Besides the thermoplastic polyimides derived from the non-coplanar benzidines, thermosetting polyimides incorporating substituted benzidines were also investigated in 1990's at the NASA Glenn Research Center. PMR-polyimide resins based on 3,3',4,4'-benzophenonetetracarboxylic acid, dimethyl ester (BTDE) and 2,2'-substituted benzidines -namely, 2,2'-bis(trifluoromethyl)benzidine (BFBZ), 2,2'-dimethylbenzidine (DMBZ), 2,2'-diphenylbenzidine (PhBZ), along with either nadic ester (NE) or 4-phenylethynylphthalic ester (PEPE) were prepared (Fig. 2). The  $T_g$ 's of these polyimides were in the range of 348-407 °C (Table 8), relatively higher than that of PMR-15 ( $T_g$  = 350 °C). The steric hindrance of 2,2'-substituted benzidine apparently generated a higher rotational barrier which was manifested in higher  $T_g$ 's in the resulting polyimides,

except for the phenyl substituents. The bulky phenyl substituents apparently disrupted the packing and resulted in a lower  $T_g$  than its counterparts. As shown in Fig. 3, the thermo-oxidative stability under isothermal aging at 288 °C for polyimides based on 2,2'-substituted benzidines followed in the decreasing order of DMBZ-PEPE > DMBZ-NE  $\approx$  PMR-15 > PhBZ-NE > BFBZ-NE. This result is surprising, since the CH<sub>3</sub> substituent is known to be oxidatively less stable than either phenyl or CF<sub>3</sub> groups in most polymers, including the corresponding BPDA based thermoplastic polyimide fibers described in the next section. Also, the CH<sub>3</sub> groups did not appear to be crosslinked during the cure as shown by solid state <sup>13</sup>C-NMR (Fig. 4) [44]. On the contrary, the PMR polyimide resins based on 4,4'-(hexafluoroisopropylidene)diphthalic acid, dimethyl ester (HFDE), BFBZ and nadic ester showed excellent thermo-oxidative stability during isothermal aging at 315 °C [45]. The use of 2,2',6,6'-tetramethylbenzidine (TMBZ) further raised the  $T_g$  of resulting polyimide, due to the increasing rotational barrier. Nevertheless, the four CH<sub>3</sub> substituents compromised its thermo-oxidative stability, because methyl groups are very susceptible to oxidative degradation at elevated temperature [46].

## 2) Composite Fabrication and Properties

i) Composite Fabrication: The monomer solutions of DMBZ-15 and PMR-15 were prepared from a 50% methanol solution of BTDE, nadic ester (NE), and MDA or DMBZ, respectively. The prepregs were made by brush application of monomer solutions onto 8 ply T650-35 carbon fabrics with UC 309 epoxy sizing in 8 harness satin weave, and subsequently dried. The laminates were cured at 315 °C (600 °F) for 2 hours by a simulated autoclave process.

ii) Composite Properties: Polyimide/T650-35 carbon fiber composite of DMBZ-15 based on BTDE, DMBZ and nadic ester in a formulated molecular weight of 1500 g/mole ( $n = 2$ ) exhibited a higher  $T_g$  (418 °C) than PMR-15 [ $T_g = 345$  °C] (Table 9), but comparable compressive strength (Fig. 5) [47] and other mechanical properties (Table 10) [48]. The higher  $T_g$  enables DMBZ-15 polyimide composite to be used for short excursions between 427- 538 °C (800-1000 °F) [49]. The restricted rotation imposed by the two CH<sub>3</sub> groups situated in *syn*-configuration (Fig. 9) on the biphenyl moiety in DMBZ diamine clearly contributed to the high  $T_g$ .

## B. Thermoplastic Polyimides Based on Substituted Benzidines

### 1) Polyimide Fibers:

Rigid-rod polyimides were prepared from 3,3',4,4'-biphenyltetracarboxylic dianhydride (BPDA) and substituted benzidines; namely, 2,2'-bis(trifluoromethyl)benzidine (BFBZ) [50, 51], 2,2'-dimethylbenzidine (DMBZ) [52] and 2,2',6,6'-tetramethylbenzidine (TMBZ) [53] by a one-step reaction in boiling m-cresol (Fig. 6). The corresponding polyimide fibers were spun from isotropic solution via a dry jet-wet spinning process to produce high strength, high modulus fibers (Table 11). These organic fibers were compared to the state-of-the-art organic fibers Kevlar® and polybenzobisoxazole (PBO, trade name Zylon®) for thermo-oxidative stability and property retention during

isothermal aging at 204 °C (Fig. 7). The BPDA-BFBZ polyimide fiber showed better property retention at elevated temperature than either Kevlar or PBO, although PBO displayed the best initial mechanical properties at room temperature [54, 55]. The polyimide fibers based on BFBZ exhibited higher thermo-oxidative stability than that of DMBZ-based polyimide fiber, due to the higher thermal stability of CF<sub>3</sub> versus CH<sub>3</sub> substituents. However, the initial tensile strength of the BPDA-BFBZ polyimide fiber was lower than that of the BPDA-DMBZ fiber, because the molecular weight of the former was lower than the latter as evidenced by the lower intrinsic viscosity of BPDA-BFBZ ( $[\eta] = 4.9$  dL/g in *m*-cresol at 30 °C) than the BPDA-DMBZ polyimide ( $[\eta] = 10$  dL/g at 60 °C in *p*-chlorophenol) as shown in Table 11. The lower reactivity of the diamine BFBZ towards the BPDA dianhydride, resulting from the electron-withdrawing effect of the CF<sub>3</sub> group as opposed to the electron-donating CH<sub>3</sub> groups, clearly contributed to the lower molecular weight in the corresponding polyimide. The glass transition temperatures ( $T_g$ 's) of these polyimides were in the increasing order of BPDA-BFBZ < BPDA-DMBZ < BPDA-TMBZ (Table 11). However, BPDA-BFBZ polyimide fiber possessed better compressive strength than either Kevlar or PBO fibers (Table 12).

## 2) Stereochemistry of Substituted Benzidines

The x-ray crystal structures of 2,2' or 2,2',6,6'-substituted benzidines [56] revealed that the two phenyl rings in BFBZ, DMBZ and TMBZ were twisted out of the coplanarity to yield dihedral angles ( $\phi$ ) of 67 °, 79 ° and 83 °, respectively (Fig. 8,9,10). These data are in contrast to the molecular modeling predictions of  $\phi = 90$  ° for 2,2'-substituted benzidines [57-59]. Furthermore, the two methyl substituents in DMBZ were situated on the same side in a *syn*-configuration as opposed to the two CF<sub>3</sub> groups located on the opposite side (*anti*-configuration). The close proximity of the two methyl groups in DMBZ clearly created a higher rotational barrier during the glass transition phase to impart the higher  $T_g$ . The four methyl substituents in TMBZ inevitably generated even more severe steric hindrance to push the two phenyl rings further out of coplanarity, as evidenced by the larger dihedral angle in TMBZ than in DMBZ. As a result, the TMBZ-based polyimide displayed higher  $T_g$  than the DMBZ-containing polyimide.

## 3) Polyimide Films

Thermoplastic films derived from 4,4'-(hexafluoroisopropylidene)diphthalic anhydride (HFDA) or pyromellitic dianhydrides (PMDA) with 2,2'-bis(trifluoromethyl)benzidine (BFBZ) have shown excellent optical transparency, low dielectric constants, low coefficients of thermal expansion (CTE) and low moisture absorption (Table 13) [60]. Polyimides derived from 1-trifluoromethyl-2,3,5,6-benzenetetracarboxylic dianhydride (P3FDA) and 1,4-bis(trifluoromethyl)-2,3,5,6-benzenetetracarboxylic dianhydride (P6FDA) with BFBZ and DMBZ have also been investigated for a similar purpose. The conclusions are summarized as follows [61]:

- 1) Introduction of CF<sub>3</sub> groups on the dianhydride units increases the CTE, but decreases the dielectric constant, the water absorption, the refractive index, the decomposition temperature and the intrinsic viscosity of the polyimides.

- 1) Polyimides with CF<sub>3</sub> substituents on the diamine (e.g. BFBZ) have lower intrinsic viscosities but higher CTE and decomposition temperature than that of CH<sub>3</sub> containing diamine (e.g. DMBZ).
- 2) The dielectric constant, the refractive index and the water absorption decrease with increasing fluorine content of the polymer.

In addition, polyimides based on 2,2'-trifluoromethoxybenzidine have shown similar characteristics, but with significantly reduced moisture absorption [62]. Furthermore, polyimides prepared from BFBZ, DMBZ and 2,2'-dihalobenzidines also displayed linear optical anisotropy which resulted in a negative birefringence that has been used in compensators for liquid crystal displays [63].

#### IV. Endcap Chemistry in Imide Oligomers

Other approaches to improve the processability of polyimides for composite applications included using imide oligomers terminated with acetylene ( $-C\equiv CH$ ) [64] and benzocyclobutane [65] as reactive crosslinking groups. However, the reactive acetylene terminal groups started to crosslink around 190-220 °C [66], very close to the melting region of imide oligomers (195-200 °C). This resulted in rapid molecular weight build-up and a very narrow processing window in systems such as the commercial Thermid Series [35]. To prevent premature curing, phenylethynyl terminated imide oligomers with 3-aminophenylethynylaniline (PEA) [67-70] and 4-phenylethynylphthalic anhydride (PEPA) endcaps [71-73] were developed to raise the curing temperature of the oligomers. Since phenylethynyl terminated oligomers usually exhibited an exothermal maximum around 350-400 °C [29] as indicated by differential scanning calorimetry (DSC), they provided a processing window about 100 °C wider than acetylene endcaps. During the 1980's, NASA Langley has successfully developed a series of phenylethynyl terminated imide oligomers (most notably, PETI-5) and other phenylethynyl pendant oligomers [74-76] for long-term (60,000 h) application at 177 °C (350 °F) in airframes. This work was supported under the High Speed Civil Transport (HSCT) program to build a Mach 2.4 supersonic commercial aircraft. PETI-5 polyimide resin is composed of 91 mole% of 3,3',4,4'-biphenyltetracarboxylic dianhydride (*s*-BPDA), 85 mole % of 3,4'-oxydianiline (3, 4'-ODA), 15 mole % of 1,3-bis(3-aminophenoxy)benzene (1,3,3-APB) and 18 mole% of 4-phenylethynylphthalic anhydride (PEPA) with a formulated oligomer molecular weight of about 5000 g/mole (Fig. 11). PETI-5 ( $T_g = 260$  °C) exhibited excellent toughness and adhesive properties (Table 14) as well as long-term mechanical property retention at 177 °C (Table 15) [77,78]. However, PETI-5 prepregs contain about 22 weight % of NMP, which often raised concerns about the volatiles and voids generated in building large airframe structures. Efforts were carried out to lower the melt viscosity of PETI-5 imidized powder to meet the requirement of resin transfer molding (RTM) by reducing the molecular weight of the oligomers [79,80] and addition of plasticizer [81] as well as changing the ratio of the monomers in PETI-5. Eventually, a solvent-free PETI-RTM resin (75% 1,3,3-APB and 25% 3,4'-ODA,  $M_n = 750$  g/mole,  $T_g = 258$  °C) that was amenable to low cost processing was demonstrated [82]. To further increase the  $T_g$  and the use temperature, modified resins formulated with *s*-BPDA, 4-phenylethynylphthalic anhydride (PEPA) along with mixed ratio of diamines of 1,3-bis(3-aminophenoxy)benzene (1,3,3-APB), 1,3-bis(4-aminophenoxy)benzene (1,3,4-

APB) and 3,5-diamino-4'-phenylethynylbenzophenone (DPEB) as a crosslinkable pendant group, (Fig. 12) were shown to exhibit low-melt viscosity ( $< 10$  poise at  $280\text{ }^{\circ}\text{C}$  for 1-2 h) that are amenable to low-cost RTM and resin infusion (RI) processes.[83]. The use of crosslinkable pendent phenylethynyl monomer (DPEB) could further raise the  $T_g$  of polyimide resins up to  $\sim 320\text{ }^{\circ}\text{C}$ , however, the increased crosslink density often led to microcracks (Table 16). Among these low-melt viscosity resins, PETI-298 ( $T_g = 298\text{ }^{\circ}\text{C}$  by DSC) displayed the best overall mechanical performance without microcracking (Table 17).

## V. Conclusions

In the polyimide field, reactive oligomers have been applied more successfully in composite applications than their thermoplastic counterparts. Using a monomer solution, the PMR approach allows the use of slightly rigid oligomers to yield crosslinked polyimides with outstanding thermo-oxidative stability for long-term (thousands of hours) applications at  $288\text{--}315\text{ }^{\circ}\text{C}$  ( $550\text{--}600^{\circ}\text{F}$ ). Recently, the incorporation of non-coplanar 4,4'-biphenyldiamines, namely 2,2'-dimethylbenzidine (DMBZ) into PMR-type polyimides raised the  $T_g$ 's to  $380\text{--}418\text{ }^{\circ}\text{C}$ ; thus, enabling the polyimide composites to be used beyond  $400\text{ }^{\circ}\text{C}$  for short-term exposure (hundreds of hours) in aerospace applications. Moreover, 2,2'-substituted benzidines have played an important role in advancing the state-of-the-art in polyamides and polyimides. These noncoplanar biphenyldiamines usually increase the solubility of the polymers, and afford optically transparent polymers by disrupting the conjugation along the backbone. They also produced unusually high birefringence in polyamide film and negative birefringence in polyimides that can be used as compensators of liquid crystal displays to increase the viewing angle. Additionally, thermoplastic polyimides containing 2,2'-substituted benzidines have been spun into high strength, high modulus fibers and found ample applications in electronics by virtue of their low coefficients of thermal expansion (CTE), low dielectric constant and low refractive index as well as low moisture absorption. The use of phenylethynyl terminated oligomers widens the processing window and yields lightly-crosslinked polyimides with excellent toughness and adhesive properties. Recent development of solvent-free phenylethynyl containing imide oligomers with low-melt viscosity ( $\sim 10$  poise at  $280\text{ }^{\circ}\text{C}$ ) enables polyimides to adapt to low-cost processes of resin transfer molding (RTM) and resin infusion (RI) commonly used for processing epoxy and bismaleimide (BMI) composites.

The future of polymer composites in light-weight aerospace components relies on the continued development of high  $T_g$  ( $\geq 350\text{ }^{\circ}\text{C}$ ) and low-melt viscosity resins (10-30 poise) that can perform at  $288\text{ }^{\circ}\text{C}$  ( $550\text{ }^{\circ}\text{F}$ ) or above from hundreds to thousands of hours in order to build light-weight structures for wide variety of applications. In addition to thermo-oxidative stability, the preferred resins also require high fracture toughness, no microcracks and good processability at reasonable material and manufacturing costs.

## ACKNOWLEDGEMENT

The author wishes to thank Dr. William B. Alston at the NASA Glenn Research Center for sharing his unpublished raw data on series of PMR polyimides that provide valuable insight towards understanding the thermo-oxidative stability of PMR polyimides.

## REFERENCES

1. Shiow-Ching Lin and Eli Pearce, High Performance Thermosets: Chemistry, Properties, Applications, Hanser Publishers, New York, 1993, pp 13-63, pp 247-266.
2. T. T. Serafini, P. Delvigs, and G. R. Lightsey, J. Appl. Polym. Sci., 16(4): 905 (1972).
3. D. Wilson, "Polyimides as Resin Matrices for Advanced Composites" in "Polyimides", Eds., D. Wilson, H. D. Stenzenberger, P. M. Hergenrother, Chapman and Hall, New York, 1990, pp 187-218.
4. J. C. Johnston, M. A. B. Meador, W. B. Alston, J. Polym. Sci., Part A: Polym. Chem., 25: 2175 (1987).
5. W. B. Alston, D. A. Scheiman, G. Sivko, High Temple Workshop XX: J-1 (2000).
6. R. W. Lauver, J. Polym. Sci., Polym. Chem., Ed., 17, 2529 (1979).
7. A. C. Wong, W. M. Ritchey, Macromolecules, 14:825 (1981).
8. D. Wilson, Brit. Polym. J., 20: 405 (1988)
9. W. B. Alston, "Cyclopentadiene Evolution during Pyrolysis-GAS Chromatography of PMR Polyimides" in Advances in Polyimide Science and Technology, Proc. of 4<sup>th</sup> Intl Conference on Polyimides, Eds. C. Feger, M. M. Khojasteh, M. S. Htoo, Technomic Publishing Co. Lancaster, PA, 1993, pp 290-310.
10. P. Iratcabal, H. Cardy, J. Org. Chem., 60: 6717 (1995).
11. M. A. B. Meador, J. C. Johnston, P. J. Cavano, Macromolecules, 30(3): (1997).
12. W. B. Alston, Polym. Prepr. (Amer. Chem. Soc., Div. Polym. Chem.), 27(2): 4410 (1986).
13. W. B. Alston, Intl. SAMPE Tech. Conf. 18: 1006 (1986).
14. P. Delvigs, Polymer Composites, 9(2):134 (1989).
15. R. D. Vannucci, K. J. Bowles, SAMPE Quarterly, 17 (2): 12 (1986).
16. R. H. Pater, Intl. SAMPE Symp., 36: 78 (1991).
17. R. H. Pater, SAMPE J., 30(5): 29 (1994).
18. R. D. Vannucci, and J. K. Chriszt, Intl. SAMPE Sym. Exhib., 40(1): 277 (1995).
19. M. A. Meador, Intl. SAMPE Sym. Exhib., 40(1): 268 (1995).
20. R. D. Vannucci, R.A. Gray, and D. S. Scheiman, HITEMP Review 1999, NASA/CP-1999-208915/ VOL 1: paper 4 (1999).
21. R. A. Gray, E. W. Collins, and Lori R. McGrath, High Temple Workshop XX: Q-1 (2000).
22. W. E. McCormack, High Temple Workshop, XVI: N-1 (1996).
23. P. Delvigs, D. L. Kopotek, and P. J. Cavano, High Perform. Polym. 9: 161 (1997).
24. P. Delvigs, D.L. Kopotek, and P. J. Cavano, High Perform. Polym. 6: 209 (1994).
25. T. T. Serafini, R. D. Vannucci, and W. B. Alston, NASA TM X-71894 (1976).
26. H. H. Gibbs, J. Appl. Polym. Sci., 35: 297 (1979).
27. R. D. Vannucci, D. C. Malarik, D. S. Papadopoulos, J. F. Waters. Intl. SAMPE Tech. Conf. 22: 175 (1990).
28. J. F. Waters, J. K. Sutter, M. A. B. Meador, L. J. Baldwin, and M. A. Meador, J.

- Polym. Sci.: Part A: Polym. Chem. 29: 1917 (1991).
29. K. C. Chuang, and J. E. Waters, Int. SAMPE Sym. & Exhib. 40(1): 1113 (1995).
  30. G. W. Myer, T. E. Glass, H. J. Grubbs, and J. E. McGrath, J. Polym. Sci.: Part A: Polym. Chem., 33: 3141(1995).
  31. B. P. Rice, HITEMP Review 1997, paper 8, NASA CP-10192 (1997).
  32. J. K. Sutter, High Temple Workshop XIV: S-1 (1994).
  33. K. J. Bowles, Int. SAMPE Tech. Conf. 20: 552 (1988).
  34. M. K. Ahn, T. C. Stringfellow, J. Lei, K. J. Bowles, M. A. Meador, Mater. Res. Soc. Symp. Pro. (High Perf. Polym. & Polym. Matrix Comp.) 305: 217 (1993).
  35. H. Stenzenberger "Chemistry and Properties of Addition Polyimides" in "Polyimides", Eds., D. Wilson, H. D. Stenzenberger, P. M. Hergenrother, Chapman and Hall, New York, 1990, pp 79-128.
  36. Shiow-Ching Lin and Eli Pearce, High Performance Thermoset Chemistry, Properties, Applications, Hanser Publishers, New York, 1993. pp188-219.
  37. T. L. St. Clair, R. A. Jewell, SAMPE Sym. and Exhib.. 23: 320 (1978).
  38. R. H. Pater, Polym. Eng. & Sci., 31(1): 14 (1991).
  39. R. H. Pater and C. D. Morgan, SAMPE J. 24(5): 25 (1988).
  40. J. P. Dosoke and J. K. Stille, ACS Org. Coat. Appl. Polym. Sci., 48: 925 (1983).
  41. H. G. Rogers, R. A. Gaudiana, W. C. Hollinsed, P. S. Kalyanaraman, J. S. Manello, C. McGrown, R. A. Minns, and R. Sahatjian, Macromolecules, 18: 1058 (1985)
  42. F. W. Harris, S. L. C. Hsu, C. C. Tso, Polym. Prepr. (Amer. Chem. Soc., Div. Polym. Chem.), 32(2): 97 (1991).
  43. T. Matsuura, N. Yamada, S. Nishi, and Y. Hasuda, Macromolecules, 26(3): 419 (1993).
  44. K. C. Chuang, M.A. B. Meador, D. Hardy-Green, "Structure-Property Relationship of Thermosetting Polyimides", Presented in Polycondensation 2000 Conference, September 18-21, Tokyo, Japan, 2000.
  45. K. C. Chuang, R. D. Vannucci, I. Ansari, L. L. Cerny, and D. A. Scheiman, J. Polym. Sci.: Part A: Polym. Chem, 32: 1341 (1994).
  46. K. C. Chuang, High Perform. Polym. 7: 81 (1995).
  47. K. C. Chuang, J. E. Waters, and DeNise Hardy-Green, Intl. SAMPE Sym. & Exhib. 42: 1283 (1997).
  48. K. C. Chuang and D. Hardy-Green, High Temple Workshop XX: P-1 (2000)
  49. F. MacDonald, P. B. Stickler, K. C. Chuang, and S. Coquill, High Temple Workshop XX: N-1 (2000).
  50. S. Z. D. Cheng, Z. Wu, M. Eashoo, S. L. C. Hsu, and F. W. Harris, Polymer, 32(10): 1803 (1991).
  51. M. Eashoo, D. Shen, Z. Wu, C. J. Lee, F. W. Harris, and S. Z. D. Cheng, Polymer, 34(15): 3209 (1994).
  52. M. Eashoo, Z. Wu, A. Zhang, D. Sheng, C. Tse, F. W. Harris, and S. Z. D. Cheng, Macromol. Chem. Phys., 195: 2207 (1994).
  53. S. Z. D. Cheng, Z. Wu, and K. C. Chuang, HITEMP Review 1995, Vol. 1, paper 6, NASA CP-10178.
  54. Zongquan Wu, Yeocheol Yoon, Frank W. Harris, Stephen Z. D. Cheng, Kathy C. Chuang, Proc. of ANTEC '96, Society of Plastic Engineers, Vol. III – Special Area May 5-10, Indianapolis, Indiana, May 5-10. Vol. III, 3038 (1996).

55. F. Li, Z.-Q. Wu, E. P. Savitski, X. Jing, Q. Fu, F. W. Harris, S. Z. D. Cheng, and R. E. Lyon, Intl. SAMPE Sym.& Exhib. 42: 1306 (1997).
56. K. C. Chuang, J. D. Kinder, D. L. Hull, D. B. McConville, and W. J. Youngs, *Macromolecules*, 30(23): 7183 (1997).
57. F. E. Arnold, Jr., K. R. Bruno, D. Shen, M. Eashoo, F. W. Harris, and S. Z. D. Cheng, *Polym. Eng. Sci.*, 46(3-4): 1373 (1996).
58. J. C. Coburn, P. D. Soper, and B. C. Auman, *Macromolecules*, 28: 3253 (1995).
59. Tsuzuki, K. Tanabe, Y. Nagawa, H. Naganishi, *J. Mol. Stru.*, 178: 7 (1988).
60. T. Matsuura, Y. Hasuda, S. Nishi, and N. Yamada, *Macromolecules*, 24(18): 5001 (1991).
61. Y. Matura, M. Ishizawa, Y. Hasuda, and S. Nishi, *Macromolecules*, 25(13): 3540 (1992).
62. A. E. Feiring, B. C. Auman, and E. R. Wonchoba, *Macromolecules*, 26(11): 2779 (1993).
63. F. L. Edward, P. Savitski, J. C. Chen, Y. Yoon, F. W. Harris, and S. Z. D. Cheng, "Linear Optical Anisotropy in Aromatic Polyimide Film and Its Application in Negative Birefringent Compensators of Liquid Crystal Displays" in *Photonic and Optoelectronic Polymer*, ACS Sym. Series 672, S. A. Jenekhe and K. J. Wynne, Eds. Am. Chem. Soc., Washington D. C., 1997, pp. 2-15.
64. Shiow-Ching Lin and Eli Pearce, *High Performance Thermosets: Chemistry, Properties, Applications*, Hanser Publishers, New York, 1993, pp 137-185.
65. Shiow-Ching Lin and Eli Pearce, *High Performance Thermosets: Chemistry, Properties, Applications*, Hanser Publishers, New York, 1993, pp 109-135.
66. T. M. Moy, C. D. Porter, and J. E. McGrath, *Polym. Prepr. (Amer. Chem. Soc., Div. Polym. Chem.)*, 33(2): 489 (1992).
67. F. W. Harris, A. Pamidimukkala, R. Gupta, S. Das, T. Wu, and G. Mock, *J. Macromol. Sci.-Chem.*, A21(869): 1117 (1984).
68. M. R. Unroe and B. A. Reinhardt, *J. Polym. Sci., Polym. Chem.*, 28, 2208 (1990).
69. C. W. Paul, R. A. Schultz, S. P. Fenelli, "High Temperature Curing End Caps for Polyimide Oligomers," in "Advances in Polyimide Science and Technology", C. Feger, M. M. Khojasteh, M. S. Htoo, Eds., Technomic Publishing Co. Inc., Lancaster, PA, 1993, pp 220-244.
70. Shiow-Ching Lin and Eli Pearce, *High Performance Thermosets: Chemistry, Properties, Applications*, Hanser Publishers, New York, 1993, pp 221-246.
71. P.M. Hergenrother and J. G. Smith, Jr., *Polymer*, 35(22): 4857 (1994).
72. J. A. Johnston, F. M. Li, F. W. Harris, and T. Takekoshi, *Polymer*, 35(22): 4865 (1994).
73. R.G. Bryant, B. J. Jensen, and P.M. Hergenrother, *J. App. Polym. Sci.*, 59(8): 1249 (1994).
74. J. W. Connell, J. G. Smith, Jr. and P. M. Hergenrother, *High Perform. Polym.*, 18(3):273 (1998).
75. J. G. Smith, J. W. Connell, and P. M. Hergenrother, *Polymer*, 389(18): 4657 (1997).
76. P. M. Hergenrother, J. W. Connell, and J. E. Smith, Jr., *Polymer*, 41: 5073 (2000).
77. R. J. Cano, and B. J. Jensen, *J. Adhesion*, 60: 113 (1997).
78. P. M. Hergenrother, *SAMPE J.*, 36(1): 30 (2000).

79. J. G. Smith, Jr., J. W. Connell, and P. M. Hergenrother, *Sci. Adv. Mat. Pro. Eng. Ser.*, 43: 93 (1998).
80. J. G. Smith, Jr., J. W. Connell, and P. M. Hergenrother, *J. Comp. Matls.* 34(7): 614 (2000).
81. J. W. Connell, J. G. Smith, Jr., P. M. Hergenrother, and M. L. Rommel, *Intl. SAMPE Tech. Conf.* 30: 545 (1998).
82. J. M. Criss, Cory P. Arendt, J. W. Connell, J. G. Smith, Jr., and P. M. Hergenrother, *SAMPE J.* 36(3): 32 (2000).
83. J. G. Smith, Jr., J. W. Connell, and P. M. Hergenrother, *Intl. SAMPE Sym. & Exhib.* 46: 510 (2001).

### List of Tables

<b>Table 1</b>	Characterization of PMR Polyimide Resins Based on BTDE and HFDA with the Nadic Endcap
<b>Table 2</b>	Properties of PMR-15 Analogs
<b>Table 3</b>	Properties of PMR-15 Analogs Containing 3-Ring Diamines
<b>Table 4</b>	Properties of PMR-15 Analogs Containing 4-Ring Diamines
<b>Table 5</b>	Second Generation PMR Polyimides Based on HFDE/ <i>p</i> -PDA/Endcap
<b>Table 6</b>	T <sub>g</sub> 's of PMR Polyimide Composites Based on HFDE/ <i>p</i> -PDA/Endcaps
<b>Table 7</b>	Mechanical Properties of Polyimide/Carbon Fiber (T650-35) Composites after Air and Nitrogen Postcure
<b>Table 8</b>	Glass Transition Temperatures (T <sub>g</sub> 's) of Polyimide Resins
<b>Table 9</b>	T <sub>g</sub> 's of PMR-15 and DMBZ-15 Polyimide/T650-35 Carbon Fiber Composites
<b>Table 10</b>	Mechanical Properties of DMBZ-15 and PMR-15 Polyimide T650-35 Carbon Fabric Composites
<b>Table 11</b>	Physical Properties of Polyimides Based on Substituted Benzidines
<b>Table 12</b>	Properties of High Mechanical Performance Organic Fibers
<b>Table 13</b>	Characterization of Polyimides based on 2,2' -Bis(trifluoromethyl)benzidine (BFBZ)
<b>Table 14</b>	Lap Shear Adhesive Strength of PETI-5
<b>Table 15</b>	IM-7/PETI-5 Laminate Properties
<b>Table 16</b>	Composition and Properties Phenylethynyl Imide Oligomers
<b>Table 17</b>	Properties of PETI-298/ AS4-5HS Carbon Fabrics

**Table 1** Characterization of PMR Polyimide Resins Based on BTDE and HFDA with the Nadic Endcap (Normalized MW =1500 g/mole)<sup>a</sup> [From Ref. 12,13]

Diamine Structure	Dianhydride Dimethyl ester	Resin Wt. Loss <sup>b</sup> @316 °C/500 hr (mg/cm <sup>2</sup> ) (BTDE / HFDE)	Composite Wt. Loss (%) <sup>b</sup> @ 316°C/400 hr (BTDE / HFDE)	T <sub>g</sub> ( °C) / Resin Postcure in Air <sup>c</sup> @ 316 °C/16 hr (BTDE / HFDE)
	BTDE/HFDE	4.97 / 5.63	1.88 / 1.56	322 / 324
	BTDE/HFDE	5.85 / 6.44	1.64 / 1.61	317 / 315
	BTDE/HFDE	5.15 / 5.67	--- <sup>d</sup> / 2.25	267 / 277
	BTDE/HFDE	6.46 / 7.74	2.74 / 2.15	269 / 260
	BTDE/HFDE	5.26 / 6.31	2.20 / ---	289 / 302
	BTDE/HFDE	8.48 / 8.75	6.64 / ---	273 / 262
	BTDE/HFDE Brittle/Brittle	12.67 / 10.67	-----	322 / 300
	BTDE/HFDE	9.51 / 6.89	3.68 / 1.91	321 / 316
	BTDE/HFDE Brittle/ ---	29.52 / 6.41	--- / 1.66	396 / 355
	BTDE/HFDE	11.03 / 11.51	3.20 / 2.77	351 / 345
	BTDE/HFDE Brittle/ ---	21.69 / 12.34	15.56 / 2.60	360 / 380
	BTDE/HFDE Brittle/ ---	38.76 / 8.12	--- / 10.15	410 / 355
	BTDE/HFDE	10.96 / 10.96	--- / ---	360 / 375
	BTDE/HFDE Brittle/ ---	12.69 / 5.16	--- / 2.13	375 / 325
	BTDE/HFDE	29.37 / 6.01	--- / 7.51	390 / 350
	HFDE	--- / 18.83	--- / ---	--- / 373

<sup>a</sup> Varied repeat unit (n) was chosen to afford a normalized molecular weight of 1500 g/mole.

<sup>b</sup> Weight loss obtained from William B. Alston's raw numerical data used in the plots for Ref. 12 and 13.

<sup>c</sup> Postcure = Resins postcured at 316 °C in air for 16 hours.

HFDE = 4,4'-(Hexafluoroisopropylidene)diphthalic acid, dimethyl ester

BTDE = 3,3',4,4'-Benzophenonetetracarboxylic acid, dimethyl ester

<sup>d</sup> --- indicated that the resin is too difficult to be processed into composites.

**Table 2** Properties of PMR-15 Analogs<sup>a</sup> [From Ref. 14, 20-22]

<div style="display: flex; justify-content: space-around; align-items: center;"> <div style="text-align: center;">   NE </div> <div style="text-align: center;">   BTDE </div> <div style="text-align: center;">   MDA </div> </div>				
Diamine Structure	Diamine	n	T <sub>g</sub> <sup>b</sup> (°C)	Composite Weight Loss (%) <sup>c</sup> @288°C/1400 hr
	MDA	2.087	345	1.52
 (RP-46)	3,4'-ODA	2.087	270	4.74
	BAPP	2	280	5.0
	BDAF	2	297 <sup>d</sup>	---
	BDAO	2	278 <sup>d</sup>	---
	Bisaniline P	2	309 <sup>e</sup>	---
	Bisaniline M	2	286 <sup>e</sup>	---

<sup>a</sup> Monomer stoichiometry : 2 NE/2 BTDE/3 diamine.

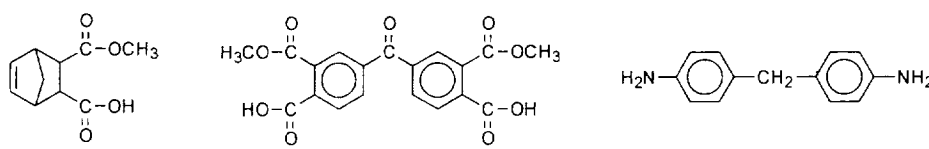
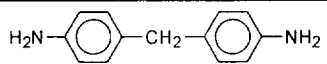
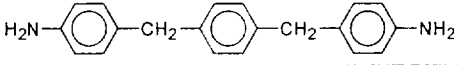
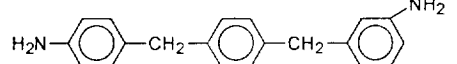
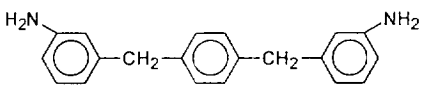
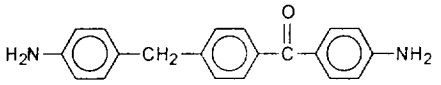
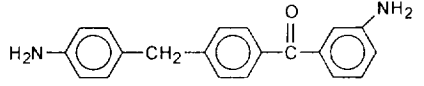
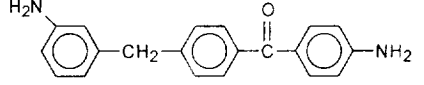
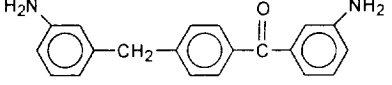
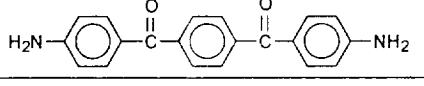
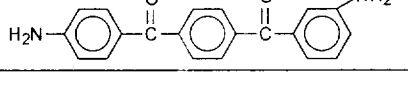
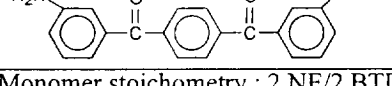
<sup>b</sup> T<sub>g</sub>'s were measured by thermal mechanical analysis (TMA) using the expansion probe with 5g load, after samples were postcured at 316 °C in air for 16 hours.

<sup>c</sup> Weight loss data were cited from ref. 22.

<sup>d</sup> T<sub>g</sub> for resins postcured at 316 °C for 24 hours in air.

<sup>e</sup> The resin disks were processed from molding powders prepared from a mixture of methanol and acetone, instead of NMP used in ref. 21 .

**Table 3** Properties of PMR-15 Analogs<sup>a</sup> Containing 3-Ring Diamines [From Ref. 23]

			
NE	BTDE	MDA	
Diamine	T <sub>g</sub> (°C)		Wt. Loss (mg/cm <sup>2</sup> ) 3024 h @ 288°C
No postcure	Postcure <sup>b</sup>		
	299	333	13.6
	268	328	13.2
	246	316	14.0
	239	278	15.6
	272	332	16.0
	249	319	17.0
	252	321	17.2
	243	298	18.5
	288	401	--- <sup>c</sup>
	269	378	--- <sup>c</sup>
	267	345	--- <sup>c</sup>

<sup>a</sup> Monomer stoichiometry : 2 NE/2 BTDE/3 diamine<sup>b</sup> Postcured in air at 316 °C for 24 h.<sup>c</sup> Unable to process the polyimide molding powders into disks.

**Table 4** Properties of PMR-15 Analogs<sup>a</sup> Containing 4-Ring Diamines [From Ref. 24]

<div style="display: flex; justify-content: space-around; align-items: center;"> <div style="text-align: center;">   NE </div> <div style="text-align: center;">   BTDE </div> <div style="text-align: center;">   MDA </div> </div>			
Diamine	T <sub>g</sub> (°C)		Wt. Loss (mg/cm <sup>2</sup> ) 3024 h @ 288°C
No postcure	Postcure <sup>b</sup>		
<b>MD</b>	299	329	11.7
<b>p-MM</b>	225	301	12.0
<b>m-MM</b>	202	253	13.4
<b>p-CM</b>	228	315	14.4
<b>m-CMC</b>	205	293	16.1
<b>p-MS</b>	217	318	13.2
<b>m-MS</b>	210	261	14.7
<b>p-CS</b>	227	323	14.9
<b>m-CS</b>	203	276	18.1
<b>p-MO</b>	225	314	18.0
<b>m-MO</b>	203	270	19.2
<b>p-CO</b>	232	321	19.4
<b>m-CO</b>	209	271	21.1

<sup>a</sup> Monomer stoichiometry : 2 NE/2 BTDE/3 diamine

<sup>b</sup> Postcured in air at 316 °C for 24 h.

**Table 5** Second Generation PMR Polyimides Based on HFDE/*p*-PDA/Endcap

Resin Name	Formulated Oligomer Structure	T <sub>g</sub> <sup>a</sup> (°C)
<b>PMR-II-50</b> FMW <sup>b</sup> = 5044		345
<b>N-CYCAP-60</b> FMW <sup>c</sup> = 4982		341
<b>V-CAP-78</b> FMW <sup>d</sup> = 7874		341
<b>PEPE-II-52</b> FMW <sup>b</sup> = 5216		362
<b>PEPE-II-78</b> FMW <sup>e</sup> = 7800		345
<b>PEA-II-75</b> FMW <sup>f</sup> = 7502		331
<b>AFR-700B</b> FMW <sup>g</sup> = 4382		380 <sup>a</sup> 405 <sup>h</sup>

<sup>a</sup> T<sub>g</sub> determined by dynamic mechanical analysis (DMA) based on the onset decline of the storage modulus (G'), using a Rheometric 800 at a heating rate of 5 °C/min in a torsional rectangular geometry at 1 Hz and 0.05% tension after specimens were postcured at 371 °C for 16 hours in air

<sup>b</sup> Monomer stoichiometry: 2 endcap/9 HFDE/10 diamine

<sup>c</sup> Monomer stoichiometry: 2 endcap/8 HFDE/9 diamine

<sup>d</sup> Monomer stoichiometry: 2 endcap/15 HFDE/14 diamine

<sup>e</sup> Monomer stoichiometry: 2 endcap/14 HFDE/15 diamine

<sup>f</sup> Monomer stoichiometry: 2 endcap/10 HFDE/9 diamine

<sup>g</sup> Monomer stoichiometry: 1 endcap/8 HFDE/9 diamine

<sup>h</sup> T<sub>g</sub> after postcure for 24 hours at 427 °C in air.

**Table 6**  $T_g$ 's of PMR Polyimide Composites Based on HFDE/*p*-PDA/Endcaps  
[From Ref. 29]

Condition	No Postcure $T_g$ (°C)		Air PC <sup>a</sup> /371°C/16h $T_g$ (°C)		N <sub>2</sub> PC <sup>b</sup> / 399°C/20h $T_g$ (°C)	
Resin	G' <sup>c</sup>	Tan $\delta$	G' <sup>c</sup>	Tan $\delta$	G' <sup>c</sup>	Tan $\delta$
PMR-II-50	332	365	346	421	408	451
V-CAP-75	322	348	341	366	397	433
PEPE-II-52	345	369	362	390	390	434
PEPE-II-78	319	352	345	379	371	410
PEA-II-75	317	342	331	388	371	432

<sup>a</sup> Air postcure = The polyimide composites were postcure in air at 371°C for 16 hrs.

<sup>b</sup> Nitrogen postcure = The polyimide composites were postcured in air at 371 °C (700 °F) for 16 hrs. followed by nitrogen postcure at 399 °C (750 °F) for 20 hrs.

<sup>c</sup> G' = The Onset decline of storage modulus.

**Table 7** Mechanical Properties of Polyimide/Carbon Fiber (T650-35) Composites after Air and Nitrogen Postcure [From Ref. 29]

Property Resin	<b>Flexural Strength (MPa)</b> 3-Point Bending			
Treatment	N <sub>2</sub> PC <sup>a</sup> /20h	N <sub>2</sub> PC/20h	N <sub>2</sub> PC <sup>b</sup> /40h	N <sub>2</sub> PC/20h
Test Temp	RT	316 °C/600°F	316 °C/600°F	371°C/700°F
PMR-II-50	1455 ± 41	862 ± 28	744 ± 50	676 ± 50
V-CAP-75	1296 ± 70	738 ± 50	703 ± 62	469 ± 4
PEPE-II-52	1317 ± 76	834 ± 80	689 ± 14	--
PEPE-II-78	1400 ± 62	910 ± 89	800 ± 28	324 ± 20
PEA-II-75	1413 ± 96	765 ± 48	717 ± 62	--
<b>Flexural Modulus (GPa)</b>				
PMR-II-50	119 ± 3	117 ± 7	97 ± 7	110 ± 14
V-CAP-75	114 ± 4	112 ± 3	103 ± 7	56 ± 3
PEPE-II-52	103 ± 6	102 ± 5	83 ± 7	--
PEPE-II-78	119 ± 3	117 ± 7	110 ± 7	32.4 ± 1
PEA-II-75	124 ± 14	97 ± 7	103 ± 14	--
<b>Short Beam Shear Strength (MPa)</b>				
PMR-II-50	79 ± 1	45 ± 3	51 ± 2	32 ± 2
V-CAP-75	70 ± 5	38 ± 3	43 ± 3	28 ± 1
PEPE-II-52	103 ± 6	43 ± 4	41 ± 7	--
PEPE-II-78	95 ± 6	48 ± 4	41 ± 7	--
PEA-II-75	96 ± 14	46 ± 3	46 ± 2	--

<sup>a</sup> The polyimide composites were postcured in air at 371 °C (700 °F) for 16 hrs followed by nitrogen postcure at 399 °C (750 °F) for 20 hrs to get optimal mechanical properties.

<sup>b</sup> The polyimide composites were postcured in air at 371 °C (700 °F) for 16 hrs. followed by nitrogen postcure at 399 °C (750 °F) for 40 hrs.

**Table 8** Glass Transition Temperatures ( $T_g$ 's) of Polyimide Resins

Resin	$T_g$ by TMA <sup>a</sup> (°C) No Postcure	$T_g$ by TMA (°C) After Postcure <sup>b</sup>
PMR-15	276	350
DMBZ-15	333	391
PEBZ-16	342	407 <sup>c</sup>
BFBZ-18	370	360 <sup>d</sup> , 404 <sup>e</sup>
PhBZ-18	250	348

<sup>a</sup> TMA = Thermal mechanical analysis by expansion probe, with 5 g load and a heating rate of 10 °C/min.

<sup>b</sup> Postcure = Air postcure at 315°C for 16 hours

<sup>c</sup> Postcured in air at 371 °C for 16 hours to complete the cure of the phenylethynyl endcap.

<sup>d</sup> 1st inflection

<sup>e</sup> 2nd inflection

**Table 9** T<sub>g</sub>'s of PMR-15 and DMBZ-15 Polyimide/T650-35 Carbon Fiber Composites<sup>a</sup> [From Ref. 47]

Property Resin	DMA <sup>b</sup> G' (onset) <sup>a</sup> , °C		DMA Tan δ, °C		TMA <sup>c</sup> (°C)	
	NPC <sup>e</sup>	APC <sup>f</sup>	NPC	APC	NPC	APC
DMBZ-15	409	414	425	430	403	420
PMR-15	345	348	375	376	320	346

<sup>a</sup> Composites were fabricated from 12 plies of unidirectional T650-35 unsized carbon fibers

<sup>b</sup> DMA = Dynamical mechanical analysis at a heating rate of 5 °C/min by a Rheometric RMS 800 instrument, using a torsional rectangular geometry at 1 Hz and 0.05% tension.

<sup>c</sup> TMA = Thermal mechanical analysis by expansion probe, with 5 g load and a heating rate of 10 °C/min.

<sup>d</sup> G' = onset decline of storage modulus.

<sup>e</sup> NPC = No postcure

<sup>f</sup> APC = Air postcure at 315 °C

**Table 10** Mechanical Properties of DMBZ-15 and PMR-15 Polyimide T650-35 Carbon Fabric Composites<sup>a,b</sup> [From Ref. 48]

Resin	DMBZ-15	PMR-15
Physical Properties		
Flexural Strength (MPa)		
23 °C ( 74 °F)	1027 ± 15 <sup>c</sup>	1082 ± 89
288 °C (550 °F)	577 ± 48	747 ± 66
371 °C (700 °F)	466 ± 32	244 ± 29
427 °C (800 °F)	193 ± 19	146 ± 5
Flexural Modulus (GPa)		
23 °C ( 74 °F)	58 ± 1	58 ± 2
288 °C (550 °F)	52 ± 1	57 ± 2
371 °C (700 °F)	52 ± 2	31 ± 2
427 °C (800 °F)	24 ± 1	16 ± 3
Short-Beam Shear Strength (MPa)		
23 °C ( 74 °F)	58 ± 4	61 ± 2
288 °C (550 °F)	45 ± 1	43 ± 2
371 °C (700 °F)	36 ± 1	25 ± 1
427 °C (800 °F)	17 ± 3	6 ± 1

<sup>a</sup> Polyimide composites were fabricated from 8 plies of T650-35, 8 harness satin weave, with UC309 epoxy sizing.

<sup>b</sup> PC = Postcured in air at 315 °C for 16 hr.

<sup>c</sup> The error bar equals one standard deviation.

**Table 11** Physical Properties of Polyimides Based on Substituted Benzidines  
[From Ref. 56]

Polyimide Property	BPDA-BFBZ	BPDA-DMBZ	BPDA-TMBZ
Intrinsic Viscosity [ $\eta$ ] (dL/g)	4.9 <sup>a</sup>	10 <sup>b</sup>	5.0 <sup>a</sup>
T <sub>g</sub> by TMA <sup>c</sup> (°C)	290	300	315
TGA/N <sub>2</sub> (5% wt loss, °C)	600	500	520
Tensile modulus (GPa)	130	150	75
Tensile Strength (GPa)	3.2	3.5	2.0
Elongation at Break (%)	4.0	4.0	2.7
Density (g/cm <sup>3</sup> )	1.45	1.40	1.37

<sup>a</sup> [ $\eta$ ] = Intrinsic viscosity determined in *m*-cresol at 30 °C (from ref 42)

<sup>b</sup> [ $\eta$ ] = Intrinsic viscosity determined in *p*-chlorophenol at 60 °C (from ref. 52)

<sup>c</sup> T<sub>g</sub> was determined by thermal mechanical analysis (TMA) on a single fiber under different stresses ( $\sigma$ ), by extrapolation to  $\sigma = 0$ .

**Table 12** Properties of High Mechanical Performance Organic Fibers [From Ref. 53]

Fiber Material	Tensile Modulus (GPa)	Tensile Strength (GPa)	Compressive Strength (MPa)
BPDA-BFBZ	130	3.2	800
Kevlar 49	130	3.6	480
PBO	365	5.8	400
Nylon	6	1.0	100

**Table 13** Characterization of Polyimides based on 2,2'-Bis(trifluoromethyl)benzidine (BFBZ) [From Ref. 60]

	HFDA-BFBZ	PMDA-BFBZ
Fluorine content (%)	31.3	23.0
Intrinsic Viscosity <sup>a</sup>	1.00	1.79
Decomp. Temp. (°C)/10% Wt. Loss in N <sub>2</sub>	569	610
Glass transition temperature (T <sub>g</sub> , °C)	335	>400
Dielectric Constant @1 Hz		
Dry	2.8	3.2
Wet (50% RH, 1 atm.)	3.0	3.6
Refractive index (λ=589.6 nm, 20 °C)	1.556	1.647
Water absorption rate (% after 3 days)	0.2	0.7
Coefficient of thermal expansion (°C <sup>-1</sup> )		
1 <sup>st</sup> run	$4.8 \times 10^{-5}$	$3 \times 10^{-6}$
2 <sup>nd</sup> run	$8.2 \times 10^{-5}$	$-5 \times 10^{-6}$

**Table 14** Lap Shear Adhesive Strength of PETI-5 [From Ref. 77]

<b>Formulated MW</b>	<b>2500 g/mole</b>	<b>5000 g/mole</b>	<b>1000 g/mole</b>
T <sub>g</sub> (cured 1hr @375 °C)	275 °C	270 °C	271 °C
Lap Shear Strength MPa (% of Cohesive Failure)			
Cured 1 hr @ 350 °C RT 177 °C	38 (70%) 31 (30%)	53 (70%) 34 (30%)	29 (20%) 20 ( 5%)
Cured 1 hr @ 375 °C RT 177 °C	40 (30%) 30 (30%)	36 (80%) 26 (80%)	14 (5%) 22 (5%)
Cured 1/2 hr@325 °C & 1/2 hr @ 375 °C RT 177 °C	45 (70%) 33 (30%)	44 (70%) 26 (50%)	29 (20%) 21 (70%)
Cured 2 hr@ 316°C RT 177 °C	45 (90%) 35 (20%)	35 (10%) 34 (50%)	29 (0%) 26 (30%)

**Table 15** IM-7/PETI-5 Laminate Properties [From Ref. 78]

Mechanical Property (Normalized to 62% fiber volume)	2500 g/mole	5000 g/mole	Lay-up
Open Hole Tension Strength (KSI) RT (dry) 177 °C (dry)	64.3 63.3	66.9 65.5	(+45, 0, -45, 90) <sub>4S</sub> (25/50/25)
Open Hole Tension Strength (KSI) RT 177 °C (dry)	83.8 82.1	80.8 81.9	(+45, -45, 90, 0, 0 +45, -45, ) <sub>S</sub> (38 / 50 / 12)
Open Hole Compression Strength (KSI) RT 177 °C (wet)	49.6 31.8	48.6 34.5	(+45, 0, -45, 90) <sub>4S</sub> (25 / 50 / 25)
Open Hole Compression Strength (KSI) RT 177 °C (wet)	54.6 38.2	53.5 42.9	(+45, -45, 90, 0, 0, +45, -45, ) <sub>S</sub> (38 / 50 / 12)
Open Hole Compression Strength (KSI) RT 177 °C (dry) 177 °C (wet)	66.5 57.3 49.9	65.3 49.7 50.0	(μ45, 0, , 0, μ45, 0, 0, , μ45, 0) <sub>2S</sub> (58 / 34 / 8)
Compression after Impact Strength (KSI) 177 °C (dry) 177 °C (wet)	47.6	45.9	(+45, 0, -45, 90) <sub>4S</sub>
Compression after Impact, Modulus (MSI) RT (dry)	8.4	8.1	(+45, 0, -45, 90) <sub>4S</sub>
Compression after Impact, microstrain (μin/in)	5908	5986	(+45, 0, -45, 90) <sub>4S</sub> (25/50/25)
0 ° Compression Strength (KSI) RT (dry)	256	241	(0) <sub>8t</sub>
0 ° Compression, Modulus (MSI) RT (dry)	19.0	19.3	(0) <sub>8t</sub>
0 ° Tension Strength (KSI) RT (dry)	342.7	332.7	(0) <sub>8t</sub>
0 ° Tension Modulus (MSI) RT (dry)	21.6	22.8	(0) <sub>8t</sub>
0 ° Tensio strain, microstrain (μin/in)	152.59	13860	(0) <sub>8t</sub>
In-Plane Shear Modulus (MSI) RT (dry) 177 °C (dry)	0.77 0.62	0.61 0.50	(0 / 100 / 0)
Interlaminar shear Strength (KSI) RT (dry)	18.8	20.6	(0) <sub>16t</sub>
Compressive Interlaminar Shear (KSI) RT (dry) 177 °C (wet)	13.9 8.6	12.5 6.8	(0) <sub>30t</sub>
Thermal Cycling Microcracks/ in. <sup>2</sup>	0	0	(μ45, 90, 00, μ45, 0, 0, μ45, 0) <sub>2S</sub> (58 / 34 / 8)

**Table 16** Composition and Properties Phenylethynyl Imide Oligomers (From Ref. 83)

Oligomer	Diamine Composition (%)	$\eta^*$ @280°C <sup>a</sup> Pa-sec	Initial T <sub>g</sub> <sup>b</sup> °C	Cure T <sub>g</sub> <sup>c</sup> °C	Microcrack Cracks/cm
PETI-RTM	1,3,3-APB (75), 3,4-ODA (25)	0.6	132	258	--
P1	1,3,3-APB (65), 3,4-ODA (15), DPEB(20)	0.4	129	295	33
P2	1,3,4-APB (100)	16	123 (246)	302	--
P3	1,3,4-APB (75), 1,3,3-APB (25)	14	134	283	--
P4(PETI-298)	1,3,4-APB (75), 3,4-ODA (25)	0.5	139	298	0
P5	1,3,4-APB (75), 3,4- ODA (15), DPEB (10)	0.6	143	313	43
P6	1,3,4-APB (85), DPEB (15)	1.0	136 (236)	320	67

<sup>a</sup> Complex melt viscosity ( $\eta^*$ ) of oligomers were measured by parallel plates at angular frequency of 100 rad/sec by Rheometrics at a heating rate of 4 °C/ min.

<sup>b</sup> Initial T<sub>g</sub> determined on oligomer powders by DSC at a heating rate of 20°C/min.

<sup>c</sup> Cured T<sub>g</sub> determined on samples held in the DSC pan at 371 °C for 1 h.

**Table 17** Properties of PETI-298/ AS4-5HS Carbon Fabrics<sup>a</sup> (From Ref. 83)

Properties	Test Temp. (°C)	PETI-298
Compression Strength (MPa)	23	421
Compression Modulus (GPa)	23	76
Open-hole Compression Strength (MPa)	23	264
Open-hole Compression Modulus (GPa)	23	45
Open-hole Compression Strength (MPa)	288	178
Open-hole Compression Modulus (GPa)	288	43
Short Beam Shear (MPa)	23	46.5
Short Beam Shear (MPa)	232	38.2
Short Beam Shear (MPa)	288	29.7

<sup>a</sup> Fabricated from unsized, AS4 Carbon fabrics, 5 harness satin weave.

### List of Figures

- Figure 1** Composition and processing of PMR-15
- Figure 2** Resin formulation of PMR polyimides based on substituted benzidines
- Figure 3** Isothermal aging of polyimide resins based on 2,2' -substituted benzidines
- Figure 4** CP-MAS  $^{13}\text{C}$  NMR of DMBZ-15 imidized powder (top) and cross-linked resin (bottom)
- Figure 5** Compressive strength of DMBZ-15 and PMR-15 composites fabricated from T650-35 carbon fabrics with UC309 epoxy sizing in 8 harness satin weave
- Figure 6** Synthesis of polyimides based on BPDA and substituted benzidines
- Figure 7** Tensile strength of high performance fibers during isothermal aging at 204 °C -- Tests were conducted using a single fiber instead of a tow
- Figure 8** X-ray crystal structure of *anti*-2,2' -bis(trifluoromethyl)benzidine (BFBZ), dihedral angle  $\phi = 67^\circ$
- Figure 9** X-ray crystal structure of *syn*-2,2' -dimethylbenzidine (DMBZ), dihedral angle  $\phi = 79^\circ$
- Figure 10** X-ray crystal structure of 2,2' ,6, 6' -tetramethylbenzidine (TMBZ), dihedral angle  $\phi = 83^\circ$
- Figure 11** Synthetic Route to PETI-5 Polyimide Resin
- Figure 12** Synthesis of phenylethynyl containing imide oligomers

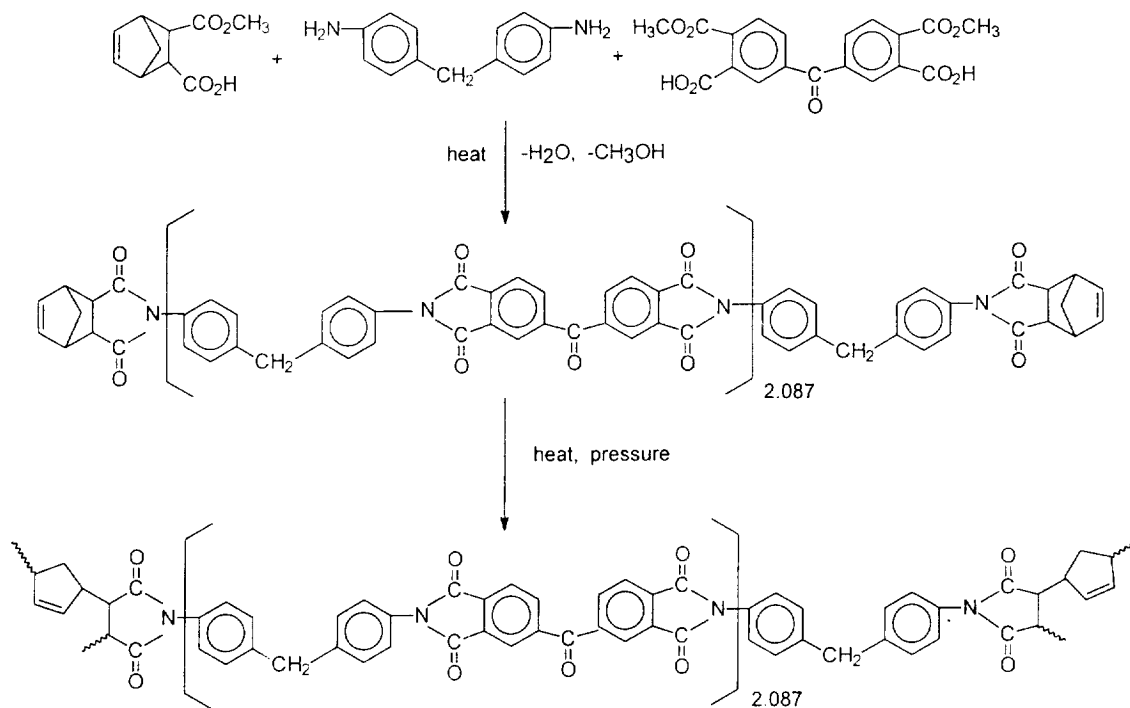


**Figure 1** Composition and processing of PMR-15

	Endcap	Dimethyl Ester	Diamine	Repeat Unit (n)
Molar Ratio	2	n	n+1	
PMR-15	 NE	 BTDE	 MDA	2.08
DMBZ-15	NE	BTDE		2
PEBZ-16	 PEPE	BTDE		2
BFBZ-18	NE	BTDE		2
PhBZ-18	NE	BTDE		2

**Figure 2** Resin formulation of PMR polyimides based on substituted benzidines

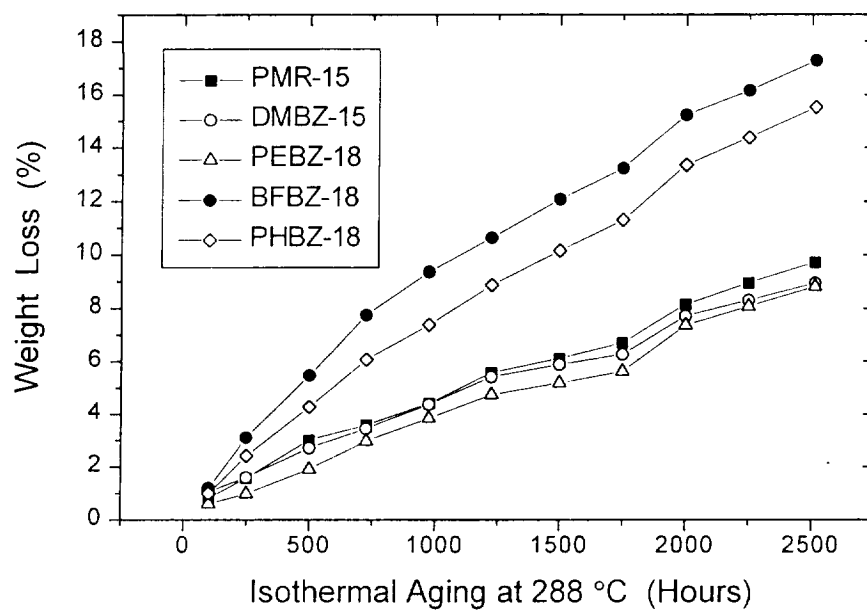


**Figure 3** Isothermal aging of polyimide resins based on 2,2'-substituted benzidines

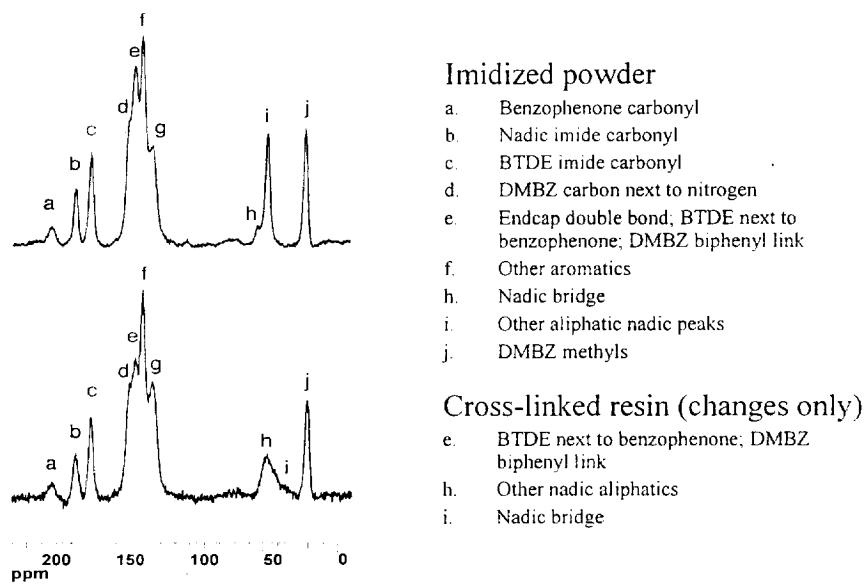


**Figure 4** CP-MAS  $^{13}\text{C}$  NMR of DMBZ-15 imidized powder (top) and cross-linked resin (bottom)

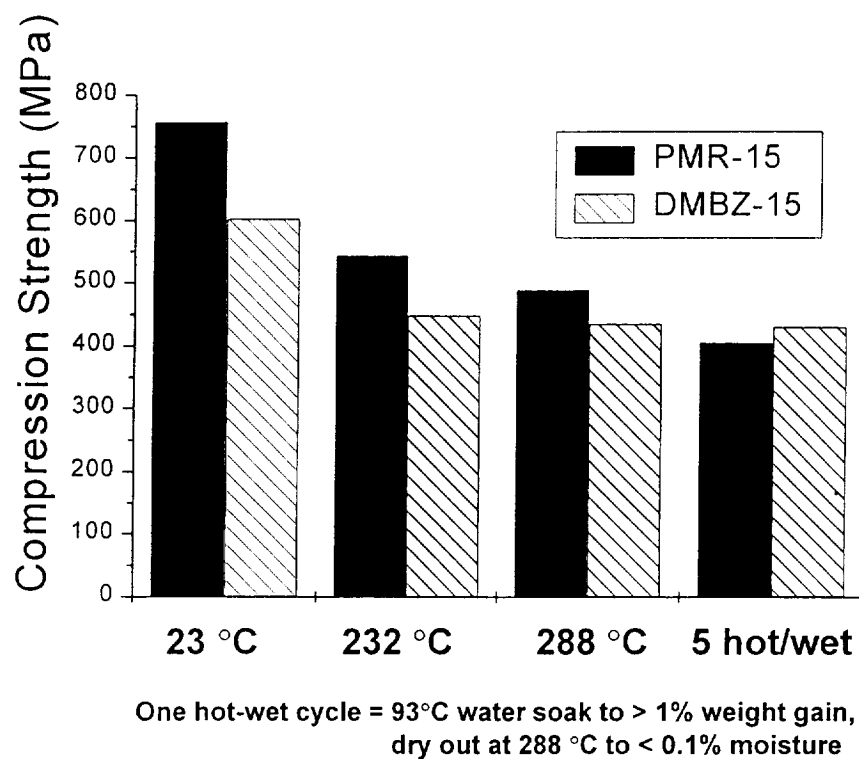


**Figure 5** Compressive strength of DMBZ-15 and PMR-15 composites fabricated from T650-35 carbon fabrics with UC309 epoxy sizing in 8 harness satin weave [47]

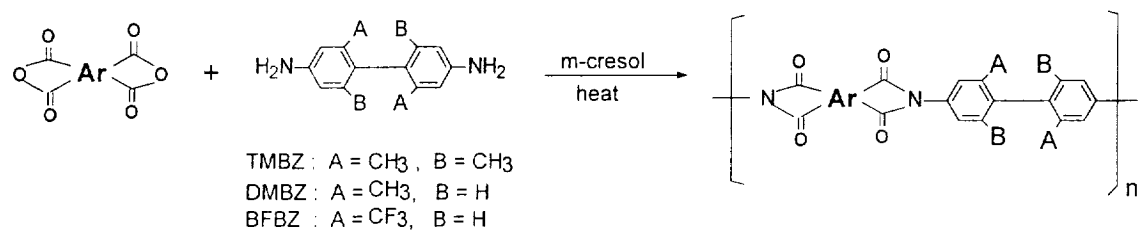


**Figure 6** Synthesis of polyimides based on BPDA and substituted benzidines

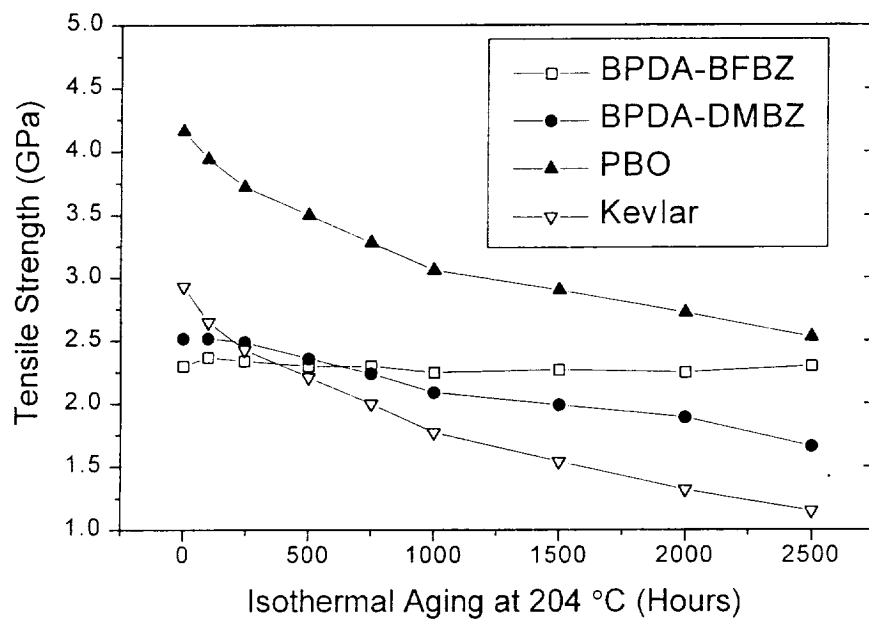


**Figure 7** Tensile strength of high performance fibers during isothermal aging at 204 °C -- Tests were conducted using a single fiber instead of a tow [From Ref. 55]

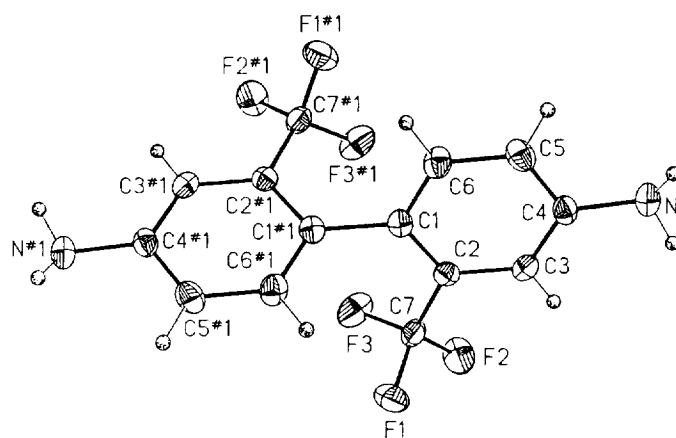


**Figure 8** X-ray crystal structure of *anti*-2,2'-bis(trifluoromethyl)benzidine (BFBZ), dihedral angle  $\varphi = 67^\circ$  [From Ref. 56]

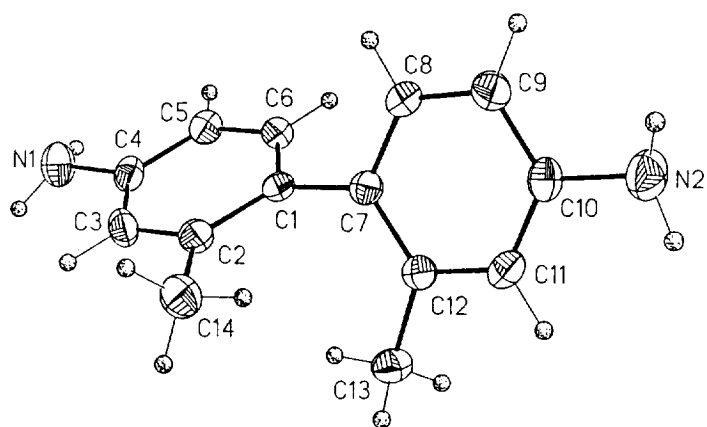


**Figure 9** X-ray crystal structure of *syn*-2,2'-dimethylbenzidine (DMBZ),  
dihedral angle  $\varphi = 79^\circ$  [From Ref. 56]

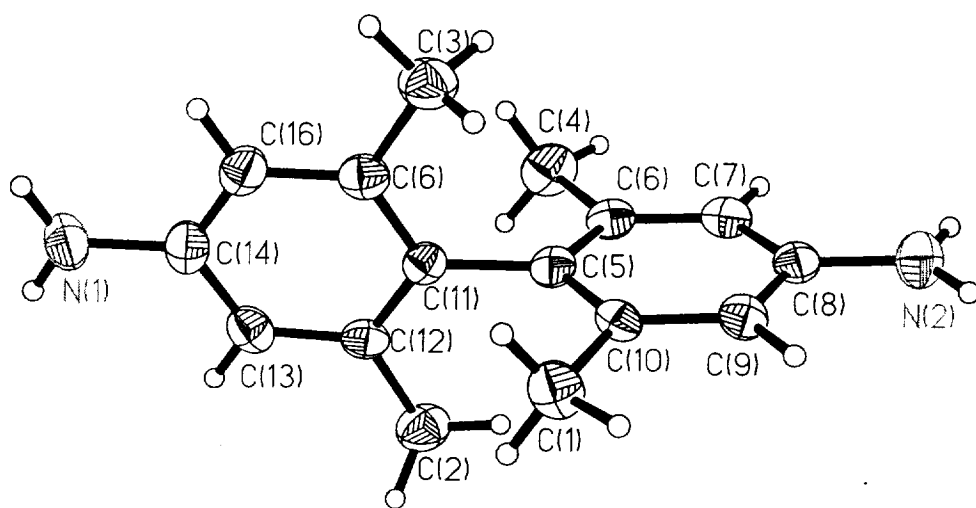


**Figure 10** X-ray crystal structure of 2,2',6,6'-tetramethylbenzidine (TMBZ),  
dihedral angle  $\varphi = 83^\circ$  [From Ref. 56]

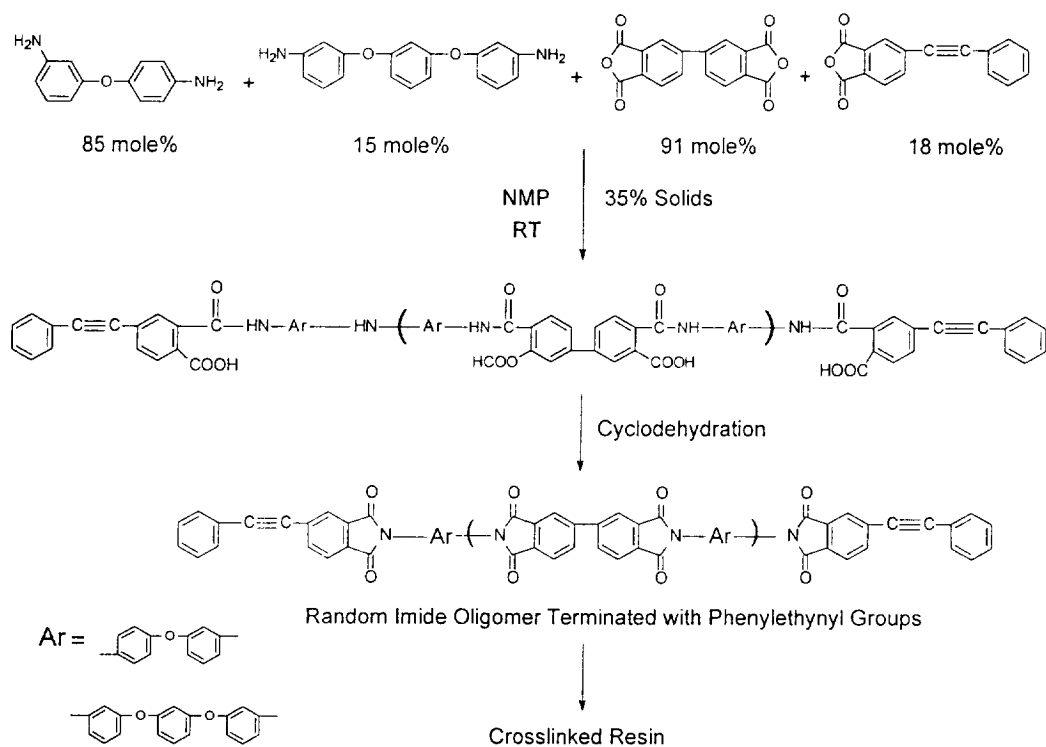


**Figure 11** Synthetic Route to PETI-5 Polyimide Resin [From Ref. 78]

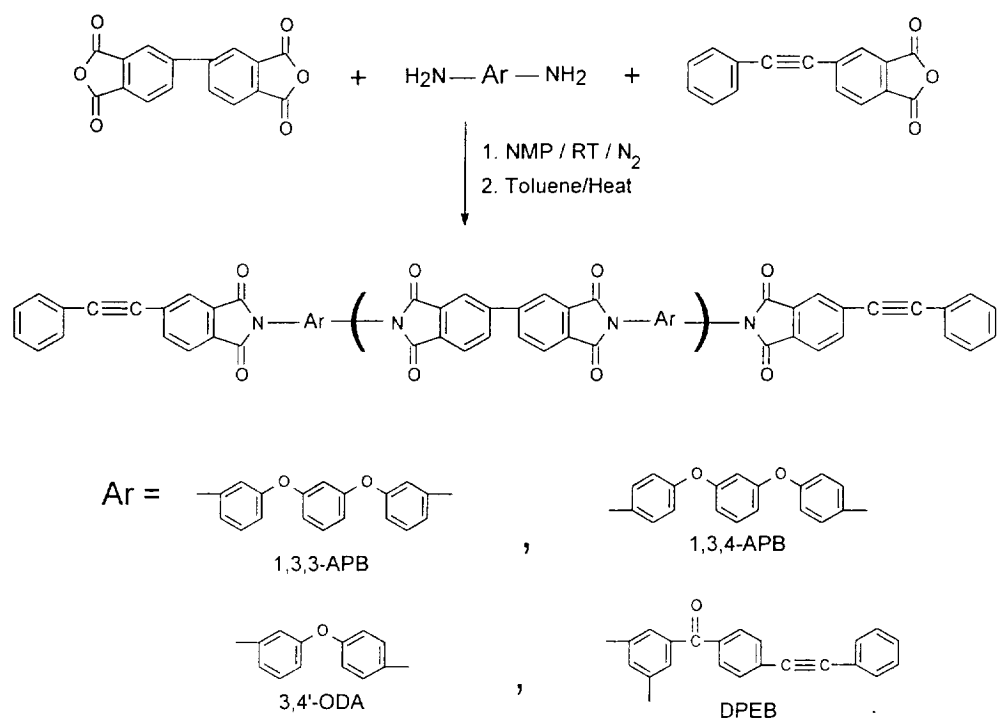


**Figure 12** Synthesis of phenylethynyl containing imide oligomers (From Ref. 83)